



The Capsule Regulatory Network of *Klebsiella pneumoniae* Defined by density-TraDISort

 Matthew J. Dorman,^a Theresa Feltwell,^a David A. Goulding,^a  Julian Parkhill,^a Francesca L. Short^{a,b}

^aWellcome Sanger Institute, Hinxton, Cambridgeshire, United Kingdom

^bDepartment of Medicine, University of Cambridge, Cambridge, United Kingdom

ABSTRACT *Klebsiella pneumoniae* infections affect infants and the immunocompromised, and the recent emergence of hypervirulent and multidrug-resistant *K. pneumoniae* lineages is a critical health care concern. Hypervirulence in *K. pneumoniae* is mediated by several factors, including the overproduction of extracellular capsule. However, the full details of how *K. pneumoniae* capsule biosynthesis is achieved or regulated are not known. We have developed a robust and sensitive procedure to identify genes influencing capsule production, density-TraDISort, which combines density gradient centrifugation with transposon insertion sequencing. We have used this method to explore capsule regulation in two clinically relevant *Klebsiella* strains, *K. pneumoniae* NTUH-K2044 (capsule type K1) and *K. pneumoniae* ATCC 43816 (capsule type K2). We identified multiple genes required for full capsule production in *K. pneumoniae*, as well as putative suppressors of capsule in NTUH-K2044, and have validated the results of our screen with targeted knockout mutants. Further investigation of several of the *K. pneumoniae* capsule regulators identified—ArgR, MprA/KvrB, SlyA/KvrA, and the Sap ABC transporter—revealed effects on capsule amount and architecture, serum resistance, and virulence. We show that capsule production in *K. pneumoniae* is at the center of a complex regulatory network involving multiple global regulators and environmental cues and that the majority of capsule regulatory genes are located in the core genome. Overall, our findings expand our understanding of how capsule is regulated in this medically important pathogen and provide a technology that can be easily implemented to study capsule regulation in other bacterial species.

IMPORTANCE Capsule production is essential for *K. pneumoniae* to cause infections, but its regulation and mechanism of synthesis are not fully understood in this organism. We have developed and applied a new method for genome-wide identification of capsule regulators. Using this method, many genes that positively or negatively affect capsule production in *K. pneumoniae* were identified, and we use these data to propose an integrated model for capsule regulation in this species. Several of the genes and biological processes identified have not previously been linked to capsule synthesis. We also show that the methods presented here can be applied to other species of capsulated bacteria, providing the opportunity to explore and compare capsule regulatory networks in other bacterial strains and species.

KEYWORDS *Klebsiella*, TraDIS, capsular polysaccharide, capsule regulation, pathogenesis

Klebsiella pneumoniae is a ubiquitous Gram-negative bacterium, found both in the environment and as an asymptomatic coloniser of the mucosal surfaces of mammals (1). *K. pneumoniae* is also an opportunistic pathogen and can express a multitude of virulence factors which enable it to cause infections in humans (1–4). Historically associated with infections in the immunocompromised and in neonates (1, 5), focus has

Received 28 August 2018 Accepted 8 October 2018 Published 20 November 2018

Citation Dorman MJ, Feltwell T, Goulding DA, Parkhill J, Short FL. 2018. The capsule regulatory network of *Klebsiella pneumoniae* defined by density-TraDISort. *mBio* 9:e01863-18. <https://doi.org/10.1128/mBio.01863-18>.

Editor Yung-Fu Chang, College of Veterinary Medicine, Cornell University

Copyright © 2018 Dorman et al. This is an open-access article distributed under the terms of the [Creative Commons Attribution 4.0 International license](https://creativecommons.org/licenses/by/4.0/).

Address correspondence to Francesca L. Short, fs13@sanger.ac.uk.

been directed on *K. pneumoniae* following the emergence of antimicrobial-resistant and hypervirulent lineages (6, 7). Hypervirulent lineages are a particular concern in a clinical setting, because they have the potential to cause infection in immunocompetent hosts (6, 8, 9), to metastasise (10), and to cause infections in unusual infection sites (11).

Numerous factors contribute to *K. pneumoniae* virulence, such as the ability to produce siderophores, fimbriae, lipopolysaccharide (LPS), and extracellular polysaccharide capsule (6, 12–14). Hypervirulence is associated with these factors, particularly with the overproduction of capsular polysaccharide (6, 12, 15, 16), and in the absence of these virulence factors, *K. pneumoniae* virulence is reduced or abolished (14, 17, 18). The ~200-kb *K. pneumoniae* virulence plasmid, which is also associated with the hypervirulent phenotype (6), encodes siderophores such as aerobactin and salmochelin and positive regulators of capsule biosynthesis (6, 19–21). More than 100 capsule locus types have been identified in *K. pneumoniae* (17), though the majority of hypervirulent *K. pneumoniae* isolates represent strains of capsule types K1 and K2 (12, 22).

Excessive capsule production is strongly associated with hypervirulence in *K. pneumoniae* (23–25), and several studies have sought to identify genetic determinants of hypervirulence. For example, the mucoviscosity-associated gene *magA* (now named *wzy_K1* [26, 27]) was originally identified by transposon mutagenesis screening (28). The *rmpA* and *rmpA2* genes also affect hypermucoviscosity and encode transcription factors that positively regulate the *K. pneumoniae* capsule biosynthesis locus (6, 15, 16, 29). These regulators can be either chromosomally encoded or plasmid-borne. Although *rmpA* is correlated with hypervirulence and strains lacking *rmpA* and aerobactin are avirulent in mice (12, 30), it has been shown that this increased virulence is a consequence of the hypermucoviscous phenotype conferred by *rmpA* rather than a consequence of the presence of the gene itself (24).

Capsule is also a potential therapeutic target in *K. pneumoniae*. Capsule-targeting monoclonal antibodies increased the killing of *K. pneumoniae* ST258 (an outbreak lineage) by human serum and neutrophils (31, 32) and limited the spread of a respiratory *K. pneumoniae* ST258 infection in mice. Specific capsule-targeting bacteriophage have been shown to clear or limit infections caused by *K. pneumoniae* strains of capsule types K1, K5, and K64 (33–35), and in some cases protection could also be achieved by treatment with the capsule depolymerase enzymes produced by these phage, rather than the phage itself. Translating these early-stage findings to the clinic is a priority as extensively drug-resistant *K. pneumoniae* strains become more prevalent (36).

Despite the absolute requirement for capsule in *Klebsiella* infections, its promise as a therapeutic target and the connection between capsule overproduction and hypervirulence and the biosynthetic and regulatory mechanisms governing *K. pneumoniae* capsule have not yet been fully explored. Genetic screens and reverse genetics (28, 37–41), including transposon mutagenesis approaches (38), have been used to identify biosynthetic genes and activators of capsule production (including the *rmpA* and *magA* genes), and some of the cues that elevate capsule expression above basal levels have also been described—these include temperature, iron availability, and the presence of certain carbon sources (12, 42). Defining the capsule regulatory network of *Klebsiella pneumoniae* in more detail not only would deepen our understanding of this pathogen's interaction with the host environment but also could inform efforts to target this factor with new therapeutics.

Here we employed transposon-directed insertion sequencing (TraDIS) (43, 44) to identify genes influencing *K. pneumoniae* capsule production. We performed density-based selection on mutant libraries of both K1 and K2 capsule type *K. pneumoniae*, using a discontinuous density gradient (45). This approach allowed the simultaneous selection of both capsulated and noncapsulated mutants from mutant libraries without requiring growth of bacteria under selective pressure. We have identified 78 genes which, when mutagenized by transposon insertion, reduce the ability of one or both of these strains to manufacture capsule. These included multiple genes not previously

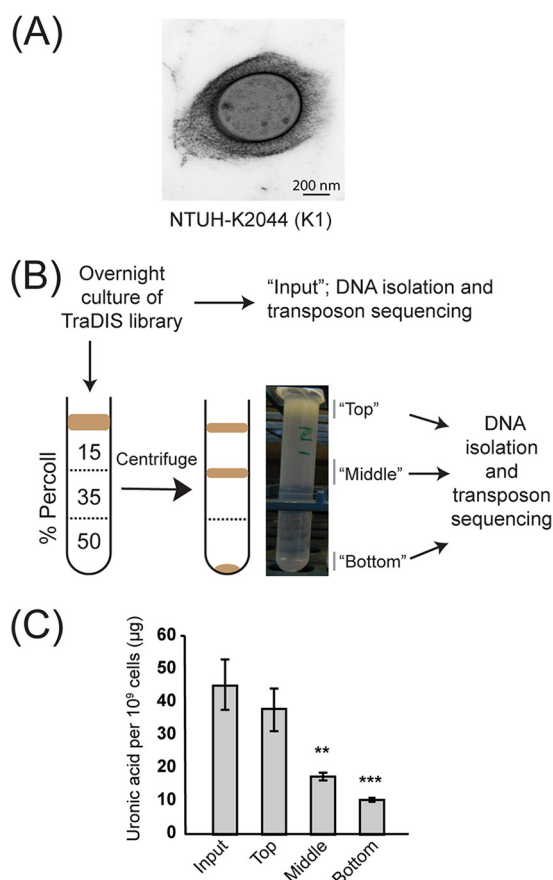


FIG 1 Summary of density-dependent TraDISort strategy. (A) Electron microscope image of capsulated *K. pneumoniae* NTUH-K2044. (B) Schematic of the density-TraDISort strategy to identify capsule regulators. A high-density transposon library is applied to the top of a discontinuous Percoll gradient, which is then centrifuged at moderate speed to separate capsulated and noncapsulated mutants. The separate fractions are sequenced to identify transposon-gDNA junctions. (C) Validation of the Percoll gradient method for separating cells by capsule phenotype. Individual fractions immediately following separation on a Percoll gradient were adjusted to an OD_{600} of 4 in sterile PBS and were assayed for uronic acid content. Statistical significance was evaluated by one-way analysis of variance (ANOVA) followed by Tukey's honestly significant difference (HSD) test, and data are reported for each fraction relative to the input sample (**, $P < 0.01$; ***, $P < 0.001$).

associated with capsule production in *K. pneumoniae*. We have also identified 26 candidate genes in NTUH-K2044 which cause an increase in capsulation when disrupted. Our results allow us to present an integrated model for capsule regulation in *K. pneumoniae* and establish a technology for study of capsule production that is applicable to other bacterial species.

RESULTS

Density gradient centrifugation separates bacterial populations on the basis of capsule phenotype. *K. pneumoniae* capsule influences the centrifugation period required to pellet cells, and this property has been used to semiquantitatively compare capsule amounts between different strains (38). On the basis of this observation, we speculated that *Klebsiella* cells of different capsulation states could be separated by density-based centrifugation and that this method could be combined with TraDIS to screen for capsule-regulating genes. Discontinuous Percoll density gradients are routinely used to purify macrophages from complex samples (46) and have also been used to examine capsulation in *Bacteroides fragilis* and *Porphyromonas gingivalis* (45, 47). Tests with *K. pneumoniae* NTUH-K2044 (capsule type K1, hypermucoid) (Fig. 1A) and *K. pneumoniae* ATCC 43816 (K2, hypermucoid) and a noncapsulated *Escherichia coli* control showed that these strains differed in density and migrated to above 15%, above

35% and below 50% Percoll, respectively (see Fig. S1A in the supplemental material). Growth of the *Klebsiella* strains at 25°C (which reduces capsule production) decreased their density, with NTUH-K2044 localizing to above 35% Percoll and ATCC 43816 showing limited migration into the 35% layer. A third *K. pneumoniae* strain, RH201207 (nonhypermuroid, capsule type K106), was retained above 50% Percoll (Fig. S1A). We also examined the proportion of *Klebsiella* bacteria migrating to different locations within the density gradient (Fig. S1B). While the majority of *K. pneumoniae* NTUH-2044 bacteria were located above the 15% layer, a small fraction (4% viable count of the top) migrated to below the interface of this layer, suggesting some heterogeneity in capsule production. In both NTUH-K2044 and ATCC 43816, only a very small number of cells were present below the 50% layer (Fig. S1B); these numbers could be partially due to cross-contamination occurring during extraction of this part of the gradient, which was recovered by pipetting from the top.

We then tested this method with a high-density transposon insertion library of *K. pneumoniae* NTUH-K2044 (generated as described in Materials and Methods). This mutant library gave rise to three fractions on a 15% to 35% to 50% Percoll gradient (Fig. 1B). The middle and bottom fractions separated from the NTUH-K2044 library contained less capsule than the input library culture, as shown by quantification of capsular uronic acids (Fig. 1C) and the hypermuroid centrifugation test (Fig. S1C). To determine whether altered migration in a Percoll gradient was the result of stable mutant phenotypes, the fractions of the *K. pneumoniae* NTUH-K2044 gradient were cultured overnight and centrifuged on a fresh gradient. The “bottom” and “top” fractions migrated to the same position as before, while the “middle” fraction showed a partially heritable phenotype and was distributed across the top and middle positions (Fig. S1D).

These data indicated that centrifugation on a discontinuous density gradient successfully separated *K. pneumoniae* populations on the basis of their capsule production and that variations in density among library mutants were, in part, due to stable phenotypes. Random-prime PCR analysis of several colonies from the bottom fraction of the *K. pneumoniae* NTUH-K2044 library identified insertions in known capsule biosynthetic or regulatory genes (see Text S1 in the supplemental material), and a *wza* insertion mutant was retained as a capsule-negative control for future experiments. We then wished to determine whether our method could be used for capsule-based separations of other species, for which we tested capsulated and noncapsulated *Streptococcus pneumoniae* 23F. These strains were separated reproducibly on a Percoll gradient (Fig. S1E), indicating that our method is applicable to other bacterial species.

Density-TraDISort identifies multiple capsule-associated genes in *Klebsiella pneumoniae*. TraDISort is a term for transposon sequencing screens that employ physical, rather than survival-based, enrichment of insertion mutants from saturated libraries (48), which allows examination of phenotypes that are not linked to survival. We call our approach “density-TraDISort” to distinguish it from the original approach using fluorescence-based flow sorting as the physical selection method. The final density-TraDISort approach is shown (Fig. 1B). Briefly, transposon mutant libraries were grown overnight at 37°C in LB, applied to the top of a Percoll gradient, and centrifuged at a moderate speed for 30 min (see Materials and Methods). Following centrifugation, each bacterial fraction was extracted and subjected to TraDIS, as was a sample of the input culture. Data were analyzed using the Bio-TraDIS pipeline (see Materials and Methods). The *K. pneumoniae* NTUH-K2044 library contained approximately 120,000 unique transposon insertion sites (equivalent to an insertion every 45 bp), with a median of 14 insertion sites per gene. Statistics summarizing the sequencing results from each fraction are reported in Table S2 in the supplemental material.

Unlike traditional growth-based transposon insertion screens, our density-TraDISort setup combines positive and negative selection within a single experiment; mutants with reduced capsule can be identified through their loss from the top fraction or by virtue of their enrichment in another fraction (see Fig. 2A for an example). We applied stringent cutoffs on the basis of both selections to identify putative capsule-related

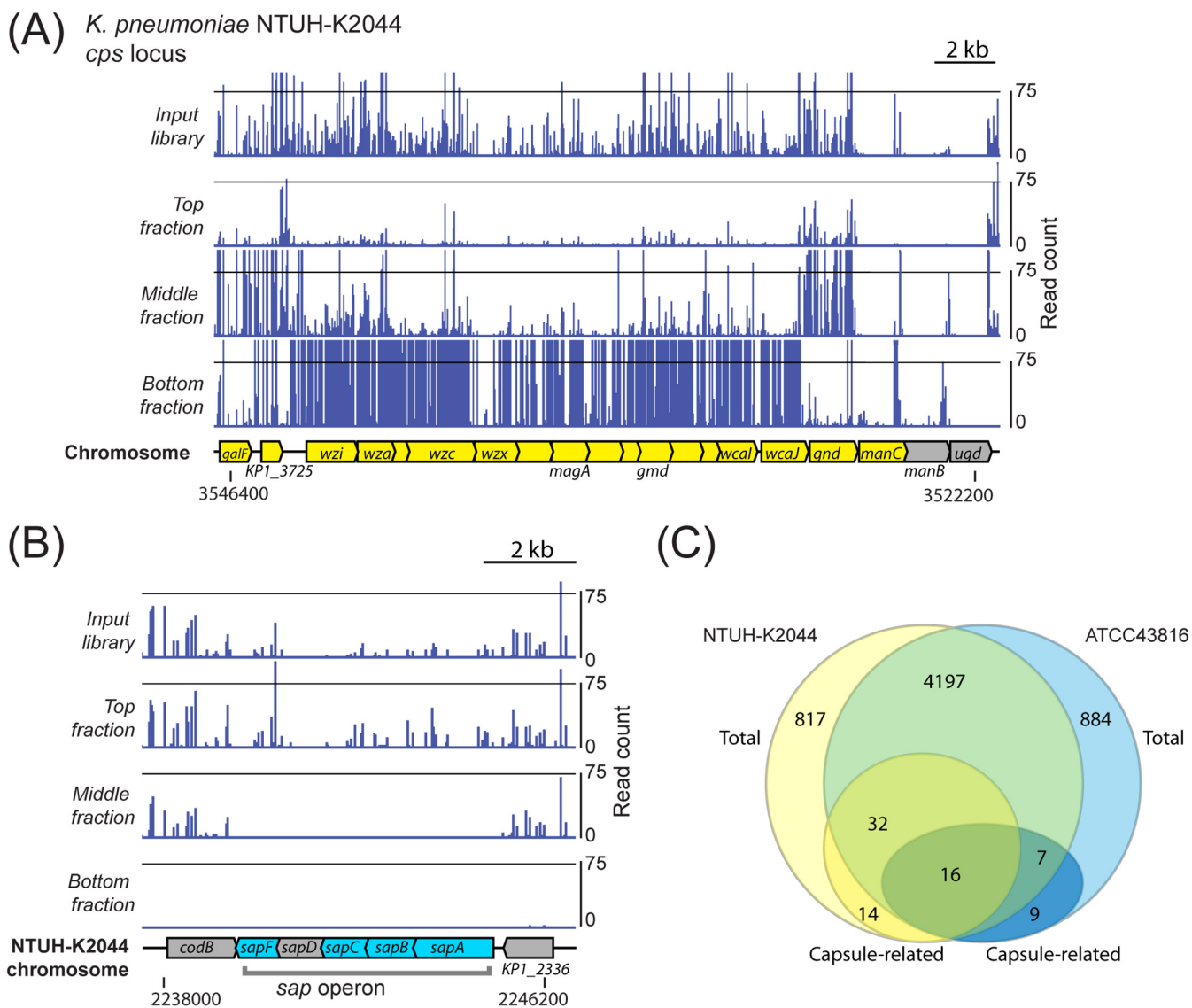


FIG 2 (A) Results of TraDIS mapping at the capsule locus of *K. pneumoniae* NTUH-K2044. Transposon insertions in capsule genes were very abundant in the input sample. The majority of these mutants were not found in the top fraction but were instead enriched in the middle fraction (e.g., *gnd* and *galF*) or the bottom fraction (all genes from *wcaJ* to *wzi*). Genes defined as hits in our screen are shown in yellow and others in gray. (B) Insertion mutations in genes of the *sap* ABC transporter locus were not found in the middle fraction, suggesting higher capsule production than wild type. Genes which are putative increased capsule hits are shown in blue, with others in gray. Note that *sapD* had a very low number of reads in all fractions. The flanking genes, *codB* and KP1_2336, are examples of genes where transposon insertion does not change capsule, and such insertion mutants were found in both the top and middle fractions. (C) Common and strain-specific genes required for full capsule production in *K. pneumoniae* NTUH-K2044 and ATCC 43816. Putative increased-capsule mutants are not considered in this chart. These two strains share approximately 4,200 genes, and the majority of genes required for full capsule production are present in both strains. Sixteen genes were defined as capsule related in both strains. Note that the gene content of the *cps* locus differs between these two strains, which accounts for the majority of hits in strain-specific genes.

genes. Briefly, a gene was counted as a hit only if it was (i) lost from the top fraction (\log_2 fold change [\log_2 FC] < -1; false-discovery-rate [q] value < 0.001) and (ii) enriched in another fraction (\log_2 FC > 1; q value < 0.001) (see Table S3 and S4). The presence of a “middle” fraction also enabled us to identify genes which increased capsulation when disrupted (an example is shown in Fig. 2B). These were apparent in the raw TraDIS plot files as genes where all or nearly all the mutants localized to the top fraction following centrifugation (mutants with wild-type capsule were distributed between the top and middle fractions, in keeping with the migration pattern of wild-type NTUH-K2044) (Fig. S1A). We defined putative “capsule up” genes as those which showed a marked depletion in the middle fraction relative to the input (\log_2 FC < -3; q value <

0.001), with genes with very low initial read counts ($\log_2\text{cpm} < 4$) excluded (Table 1; see also Table S4). Examples of TraDISort data for several genes known to affect capsule production are shown in Fig. S2C.

In total, we identified 62 genes required for full capsule production in *K. pneumoniae* NTUH-K2044 (Table 1; see also Table S4). We also identified 26 putative capsule up mutants in this strain (Table 1; see also Table S4). The biological roles of the genes determined to influence capsule production are discussed in more detail below.

Global regulators, metabolic genes, and cell surface components affect capsule in *K. pneumoniae*. Our “capsule down” mutants included almost every gene of the capsule biosynthesis locus of *K. pneumoniae* NTUH-K2044 (Fig. 2A), further confirming that our experimental strategy had successfully isolated capsule-deficient mutants. The *manB* and *ugd* genes were not called as hits, however, these contained very few insertions in the input sample (visible in the plot files above these genes in Fig. 2A). In addition to biosynthetic genes, the known capsule regulators *rpmA*, *rdsB*, and *rfaH* were identified (Fig. S2C).

Other capsule down hits included multiple cell surface components, metabolic genes, and genes of global regulatory systems. Extended functional information corresponding to all of our hits, including reported links to capsule production in *Klebsiella* and other proteobacteria, is included in Table S4. Gene enrichment analysis using the TopGO package (49) indicated that genes for polysaccharide metabolic processes ($P = 1.7 \times 10^{-5}$), molecular transducers ($P = 0.0042$), and protein kinases ($P = 0.005$) were overrepresented in our hits (all probabilities are from Fisher's exact test, parent-child algorithm [50]).

Several global regulators were identified as affecting capsule production. These included the ArcB anaerobic/redox-sensitive sensor kinase, the OmpR-EnvZ osmotic stress response system, the BarA-UvrY system, the ArgR arginine repressor, and the CsrB carbon storage regulatory small RNA. Transcription regulators MprA and SlyA were also needed for full capsule production. Metabolic genes, including genes coding for the electron transport chain, glycolytic enzymes, and the GlnB nitrogen source regulatory protein, were also identified.

The capsule up mutants of NTUH-K2044 included nucleoid proteins, membrane-bound transporters such as SapBCDF (Fig. 2B), and several metabolic gene products (Table S4). Interestingly, some of the capsule up hits, including CsrD (targets CsrB for degradation), H-NS (reported to be antagonized by SlyA), and GlnD (modifies and controls activity of GlnB), are known antagonists or regulators of genes in the capsule down hits.

Finally, our results also included many genes for other cell surface components; genes for the synthesis and modification of LPS were identified, along with enterobacterial common antigen (ECA) genes and the Lpp lipoprotein gene.

Distinct and overlapping capsule regulators in two *K. pneumoniae* strains. We wished to determine the extent of conservation of our capsule-regulatory hits across the *Klebsiella* species, and the overlap of the capsule-influencing genes in different *Klebsiella* strains. To explore this issue, we applied our density-TraDISort method to a second strain, *K. pneumoniae* ATCC 43816, a capsule type K2 strain which is commonly used in *Klebsiella* infection studies (Fig. S3A). We constructed a *K. pneumoniae* ATCC 43816 saturated transposon insertion library with ~250,000 unique insertion sites (or an insertion every 22 bp) and a median of 36 insertion sites per gene (see Materials and Methods) (Fig. S3C and D). This library resolved into two fractions on a 35% to 50% Percoll gradient, with no obvious heritable “middle” fraction, and fractions were collected and their transposon insertion junctions sequenced as described for *K. pneumoniae* NTUH-K2044. Genes were counted as hits in this strain if they were lost from the top fraction relative to the input ($\log_2\text{FC} < -1$; q value < 0.001) and enriched in the bottom fraction ($\log_2\text{FC} > 1$; q value < 0.001). The lack of a “middle” fraction in this experiment meant that there was less sensitivity for identifying reduced-capsule mutants, particularly using the second, positive-selection-based filtering criterion. We

TABLE 1 Genes in which mutants have altered capsule production^a

Gene	Annotation	Proportion of strains	Locus tag ^c	
			NTUH-K2044	ATCC 43816
Low-capsule mutants				
<i>wzxE</i>	WzxE protein	0.94	KP1_0154	VK055_3183
<i>wzy</i>	ECA polymerase	1.00	KP1_0156	VK055_3181
<i>rfaH</i>	Transcriptional activator RfaH	1.00	KP1_0199	VK055_3141
<i>seqA</i>	Replication initiation regulator SeqA	0.99	KP1_1663	VK055_1821
<i>pgm</i>	Phosphoglucomutase	1.00	KP1_1664	VK055_1820
<i>gnd</i>	6-Phosphogluconate dehydrogenase	0.69	KP1_3704	VK055_5026
<i>wcaJ</i>	Colanic acid biosynthesis UDP-glucose lipid carrier transferase WcaJ	0.20	KP1_3705	VK055_5025
<i>wza</i>	Polysaccharide export protein	0.98	KP1_3720	VK055_5015
<i>wzi</i>	Outer membrane protein	0.99	KP1_3721	VK055_5014
<i>orf2</i>	PAP2 family protein	0.93	KP1_3725	VK055_5013
<i>mldD</i>	ABC transporter	1.00	KP1_4915	VK055_3874
<i>arnF</i>	4-Amino-4-deoxy-L-arabinose-phosphoundecaprenol flippase subunit ArnF	1.00	KP1_5178	VK055_3630
<i>arnE</i>	SMR family multidrug resistance protein	0.95	KP1_5179	VK055_3628
<i>arnD</i>	Polymyxin resistance protein PmrJ	1.00	KP1_5181	VK055_3626
<i>gor</i>	Glutathione reductase	1.00	KP1_5206	VK055_3604
<i>wabN</i>	Deacetylase	1.00	KP1_5319	VK055_3502
<i>wecA</i>	Undecaprenyl-phosphate N-acetylglucosaminyl 1-phosphate transferase	0.98	KP1_0146	VK055_3191
<i>yjeA</i>	Translation elongation factor P Lys34:lysine transferase	1.00	KP1_0426	VK055_2911
<i>miaA</i>	tRNA delta(2)-isopentenylpyrophosphate transferase	1.00	KP1_0439	VK055_2895
<i>dkcA</i>	RNA polymerase-binding transcription factor	0.99	KP1_0973	VK055_2423
<i>htpG</i>	Chaperone protein HtpG	0.97	KP1_1331	VK055_2094
<i>manA</i>	Mannose-6-phosphate isomerase	0.65	KP1_2524	VK055_0991
<i>ydgl</i>	Arginine/ornithine antiporter ArcD	1.00	KP1_2534	VK055_0982
<i>rnfA</i>	Electron transport complex protein RnfA	0.98	KP1_3036	VK055_0514
<i>rnfC_2</i>	Electron transport complex protein RnfC	0.38	KP1_3038	VK055_0512
<i>nqrB_1 (rnfD)</i>	Electron transport complex protein RnfD	0.99	KP1_3039	VK055_0511
<i>rnfE</i>	Electron transport complex protein RnfE	0.78	KP1_3041	VK055_0509
<i>slyA_1</i>	Transcriptional regulator SlyA	1.00	KP1_3054	VK055_0496
<i>lpp</i>	Major outer membrane lipoprotein	1.00	KP1_3230	VK055_0326
<i>galU</i>	UTP-glucose-1-phosphate uridylyltransferase	0.97	KP1_3315	VK055_0250
<i>uvrY</i>	BarA-associated response regulator UvrY (GacA, SirA)	1.00	KP1_3542	VK055_0032
<i>rmpA</i>	Regulator of mucoid phenotype	0.05	KP1_3619	VK055_5097
<i>manC</i>	Mannose-1-phosphate guanylyltransferase	0.24	KP1_3703	VK055_5027
<i>galF</i>	UDP-glucose pyrophosphorylase	0.88	KP1_3726	VK055_5012
<i>rcsB</i>	DNA-binding capsular synthesis response regulator RcsB	0.77	KP1_3872	VK055_4883
<i>glnB</i>	Nitrogen regulatory protein P-II	1.00	KP1_4132	VK055_4623
<i>rluD</i>	23S rRNA pseudouridine synthase D	0.96	KP1_4172	VK055_4583
<i>emrR</i>	Transcription repressor	1.00	KP1_4277	VK055_4504
<i>barA</i>	BarA sensory histidine kinase	0.92	KP1_4400	VK055_4386
<i>greA</i>	Transcription elongation factor GreA	0.99	KP1_4900	VK055_3886
<i>arcB</i>	Aerobic respiration control sensor protein arcB	1.00	KP1_4931	VK055_3858
<i>argR</i>	Arginine pathway regulatory protein ArgR	1.00	KP1_4961	VK055_3832
<i>envZ_2</i>	Osmolarity sensory histidine kinase EnvZ	0.90	KP1_5105	VK055_3697
<i>ompR</i>	Osmolarity response regulator	1.00	KP1_5106	VK055_3696
<i>rfaZ</i>	Lipopolysaccharide core biosynthesis protein RfaZ	0.76	KP1_5316	VK055_3505
<i>waal</i>	O-Antigen polymerase	0.78	KP1_5317	VK055_3504
<i>rfaQ (waaQ)</i>	Lipopolysaccharide heptosyltransferase III	1.00	KP1_5320	VK055_3501
<i>wabH</i>	Glycosyltransferase	1.00	KP1_5322	VK055_3499
<i>yjeK</i>	EF-P beta-lysylation protein EpmB	NA	KP1_0415	NA
<i>wcaI</i>	Putative glycosyl transferase	0.11	KP1_3706	NA
<i>gmm (wcaH)</i>	GDP-mannose mannosyl hydrolase	0.05	KP1_3708	NA
<i>wcaG</i>	GDP-fucose synthetase	0.11	KP1_3709	NA
<i>gmd</i>	GDP-mannose 4,6-dehydratase	0.13	KP1_3711	NA
<i>KP1_3712</i>	Galactoside O-acetyltransferase	0.00	KP1_3712	NA
<i>group_19979</i>	Glycosyltransferase	0.06	KP1_3713	NA
<i>magA</i>	Mucoviscosity-associated protein	0.06	KP1_3714	NA
<i>KP1_3715</i>	Polysaccharide pyruvyl transferase	0.05	KP1_3715	NA
<i>wzx</i>	Repeat unit exporter	0.06	KP1_3716	NA
<i>wzc</i>	Tyrosine-protein kinase Wzc	0.06	KP1_3718	NA
<i>wzb</i>	Putative protein tyrosine phosphatase	0.00	KP1_3719	NA
<i>csrB^b</i>	Carbon storage regulatory sRNA	NA	KP1_6106	NA
<i>rmpA_2^b</i>	Regulator of mucoid phenotype	NA	KP1_p020	NA
<i>pgi</i>	Glucose-6-phosphate isomerase	1.00	KP1_0264	VK055_3061
<i>mioC_2</i>	Flavodoxin	0.99	KP1_0001	VK055_3326
<i>glpD</i>	Aerobic glycerol-3-phosphate dehydrogenase	0.99	KP1_5126	VK055_3679
<i>yrbF</i>	Putative ABC transporter ATP-binding protein YrbF	1.00	KP1_4917	VK055_3872
<i>mldE (yrbE)</i>	ABC transporter	1.00	KP1_4916	VK055_3873
<i>mldC (yrbC)</i>	ABC transporter	1.00	KP1_4914	VK055_3875
<i>mldA</i>	lipoprotein	1.00	KP1_3977	VK055_4786
<i>wzb</i>	Putative acid phosphatase Wzb	0.01	NA	VK055_5016

(Continued on next page)

TABLE 1 (Continued)

Gene	Annotation	Proportion of strains	Locus tag ^c	
			NTUH-K2044	ATCC 43816
<i>wzc (etk)</i>	Tyrosine autokinase	0.08	NA	VK055_5017
<i>mshA</i>	Group 1 glycosyl transferase	0.08	NA	VK055_5018
<i>orf8</i>	Group 1 glycosyl transferase	0.08	NA	VK055_5019
<i>VK055_5020</i>	Group 1 glycosyl transferase	0.08	NA	VK055_5020
<i>VK055_5021</i>	Lipid A core-O-antigen ligase and related enzymes	0.08	NA	VK055_5021
<i>wzxC</i>	Colanic acid exporter	0.08	NA	VK055_5022
<i>orf12</i>	Hypothetical protein	0.08	NA	VK055_5023
<i>orf13</i>	Putative lipopolysaccharide biosynthesis O-acetyl transferase WbbJ	0.06	NA	VK055_5024
High-capsule mutants				
<i>polA</i>	DNA polymerase I	0.79	KP1_0024	
<i>cyaA</i>	Adenylate cyclase	0.99	KP1_0164	
<i>trkH</i>	Potassium transport protein	1.00	KP1_0206	
<i>purA</i>	Adenylosuccinate synthetase	1.00	KP1_0448	
<i>apaH</i>	Diadenosinetetraphosphatase	0.96	KP1_0859	
<i>ace</i>	Pyruvate dehydrogenase E1 component	0.98	KP1_0941	
<i>glnD</i>	Pil uridylyl-transferase	0.94	KP1_1019	
<i>hha</i>	Hemolysin expression modulating protein	0.99	KP1_1317	
<i>tolR</i>	Putative inner membrane protein involved in the <i>tonB</i> -independent uptake of group A colicins	1.00	KP1_1700	
<i>tolB</i>	Translocation protein TolB precursor	1.00	KP1_1702	
<i>mdoG</i>	Periplasmic glucans biosynthesis protein	1.00	KP1_2050	
<i>mdoH</i>	Glucosyltransferase	0.93	KP1_2051	
<i>sapF</i>	ABC-type peptide transport system ATP-binding component	0.97	KP1_2331	
<i>sapC</i>	ABC-type peptide transport system permease component	1.00	KP1_2333	
<i>sapB</i>	ABC-type peptide transport system permease component	0.99	KP1_2334	
<i>sapA</i>	ABC-type peptide transport system periplasmic component	0.68	KP1_2335	
<i>pykF</i>	Pyruvate kinase	0.99	KP1_3229	
<i>hns</i>	DNA-binding protein HLP-II/pleiotropic regulator	0.99	KP1_3314	
<i>prc</i>	Carboxy-terminal protease for penicillin-binding protein 3	0.11	KP1_3473	
<i>ackA</i>	Acetate/propionate kinase	1.00	KP1_3933	
<i>pta</i>	Phosphate acetyltransferase	0.80	KP1_3934	
<i>smpB</i>	SsrA tmRNA-binding protein	1.00	KP1_4198	
<i>ptsN</i>	Sugar-specific PTS family enzyme IIA component	1.00	KP1_4926	
<i>KP1_4976 (csrD)</i>	<i>csrB</i> regulatory protein CsrD	0.95	KP1_4976	
<i>fis</i>	DNA-binding protein	1.00	KP1_4989	
<i>pitA</i>	Putative low-affinity inorganic phosphate transporter	0.84	KP1_5198	

^aA list of all statistically significant genes from this TraDIS screen which, when disrupted by transposon insertion, increase capsule production in *K. pneumoniae*. Cutoff criteria are described in Materials and Methods. Gene names and functional annotations are taken from the pan-genome consensus file (see Materials and Methods). The complete data set, including statistical data, is provided in Table S3 and S4.

^bNote that the pan-genome includes only protein-coding sequences located on the chromosome, so the small RNA *csrB* gene and plasmid-encoded *rmpA2* gene are not included in our pan-genome analysis.

^cLocus tags are shown in bold for hits and in italics where the gene was not called as a hit.

used a pan-genome generated from 263 annotated *K. pneumoniae* genomes (Table S5) to define the common genes in NTUH-K2044 and ATCC 43816 and to determine their prevalence across the *K. pneumoniae* population (Table 1; see also Table S4).

We identified 34 candidate capsule-regulatory genes in *K. pneumoniae* ATCC 43816. As observed for NTUH-K2044, the genes of the capsule biosynthetic locus were nearly all called as hits (Fig. S3E). Of the three genes that were not, two had very low initial insertion counts, and the third met our first selection criterion of being lost from the top fraction but was not enriched in the bottom fraction. Putative capsule-influencing genes of ATCC 43816 fell into diverse functional categories, with genes encoding cell surface components, metabolic genes, and genes associated with transporters and known regulators implicated.

Although the majority of capsule hits are encoded in the core genome (48 of 62 in *K. pneumoniae* NTUH-K2044; 23 of 32 in *K. pneumoniae* ATCC 43816; Fig. 2C), only 16 genes were called as hits in both strains. These shared genes included five shared components of the two strains' capsule biosynthesis loci, the transcription antiterminator *rfaH*, two enterobacterial common antigen genes, three genes of the *arn* operon responsible for modification of LPS lipid A with L-Ara4N, and the glutathione reductase *gor* gene. Strain-specific differences were also identified, with the caveat that NTUH-K2044 produces more capsule (Fig. S3B) and therefore afforded us greater sensitivity in our experiment. Genes that were identified as required for ATCC 43816 capsule

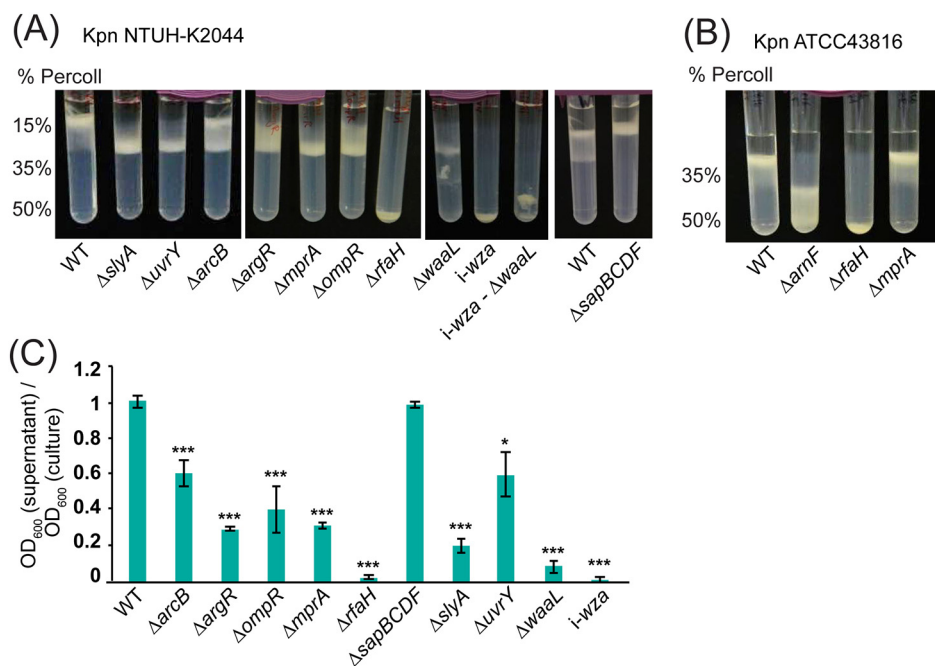


FIG 3 Validation of putative capsule regulators with single-gene-deletion mutants. (A) Percoll gradient centrifugation of clean deletion mutants in selected NTUH-K2044 genes. All of the genes tested showed reduced density compared to the wild type (WT), with the exception of the putative increased-capsule mutant, Δ sapBCDEF, which stayed above the 15% Percoll layer. (B) Validation of ATCC 43816 deletion mutant phenotypes on 35% to 50% Percoll gradients. The Δ arnF and Δ rfaH mutants showed reduced density compared to the wild type, while the Δ mprA mutant did not, in contrast to its phenotype in NTUH-K2044. (C) Hypermucoidity tests with *K. pneumoniae* NTUH-2044 mutants. Strains were grown to late stationary phase and cultures centrifuged for 5 min at $1,000 \times g$. The OD₆₀₀ of the supernatant was measured and is presented here as a proportion of the starting OD₆₀₀. *, $P < 0.05$; ***, $P < 0.001$ (one-way ANOVA followed by Tukey's HSD test, relative to the wild type).

production but not NTUH-K2044 capsule production included the *yrcCDEF* (*mIaCDEF*) ABC transporter genes and the *mIaA* gene, which are involved in maintaining outer membrane asymmetry through the cycling of phospholipids (51). Thirty-two genes common to both strains had a capsule down phenotype in NTUH-K2044 but were not called as hits in ATCC 43816 (note that capsule up hits are not included in our comparison as these were not resolved in ATCC 43816). These included electron transport pump *rnf*, global regulators such as *arcB* and *ompR*, transcription factor *mprA*, and several additional cell surface component biosynthetic genes. It appears that the influence of at least some conserved genes on capsule is strain specific.

Phenotypes of single-gene mutants confirm results of density-TraDISort. We generated a set of 10 single-gene-deletion mutants in *K. pneumoniae* NTUH-K2044, and a set of 3 in *K. pneumoniae* ATCC 43816, in order to validate the results of our density-TraDISort screen. Genes selected for mutagenesis were the known capsule and LPS regulator gene *rfaH* in both strains, the LPS O-antigen ligase gene *waal*, the aerobic respiration control sensor gene *arcB*, and multiple transcriptional regulator genes (*ompR*, *argR*, *slyA*, *mprA*, and *uvrY*). We also deleted the *arnF* gene in ATCC 43816. The *sapBCDF* ABC transporter in NTUH-K2044 was examined in order to validate our assignment of capsule up hits.

Single-gene-knockout mutants were grown under the same conditions as in the original screen and were subjected to density gradient centrifugation. Every mutant showed a banding pattern consistent with the results of density-TraDISort (Fig. 3A and B). The Δ arcB mutant appeared to have two populations, one with wild-type capsule and one with reduced capsule. Most of the other NTUH-K2044 mutants migrated to the position of the middle fraction, while the Δ waal, *i-wza*, and Δ rfaH mutants migrated to the bottom of the gradient. The Δ sapBCDF mutant showed higher density than the wild-type strain and remained above the 15% Percoll layer, with no movement into the

gradient itself. Mutants of NTUH-K2044 were also tested for hypermucoidity and uronic acid production, and these experiments showed increased capsule in NTUH-K2044 $\Delta sapBCDF$ and reduced capsule in all other mutants (Fig. 3C; see also Fig. S4B). Of the *K. pneumoniae* ATCC 43816 mutants (Fig. 3B), the $\Delta rfaH$ mutant migrated to the bottom of the gradient and the $\Delta arnF$ mutant to the middle and bottom, while mutant $\Delta mprA$ showed the same pattern as the wild type. This is consistent with the TraDISort assignment of this gene as having a strain-specific effect on capsule, at least under these growth conditions (Table 1).

Our hits included several genes with roles in LPS biosynthesis, which raised the possibility that LPS O-antigen may affect cell density independently of capsule. To test this possibility, we constructed a $\Delta waal$ deletion in our *wza* transposon insertion strain (see Materials and Methods). The resulting double mutant had no detectable reduction in density compared to the *wza* mutant on the standard 15% to 35% to 50% gradient or on 70% Percoll (representing the minimum concentration required to exclude the *wza* mutant; Fig. S4A), indicating that the LPS O-antigen alone does not affect the density of *K. pneumoniae*, at least within the resolution range of this experiment.

Virulence and capsule architecture of *K. pneumoniae* NTUH-K2044 $\Delta argR$, $\Delta mprA$, $\Delta sapBCDF$, and $\Delta slyA$. We selected the transcription factors ArgR, SlyA, and MprA, along with the ABC transporter SapBCDF, for further characterization. ArgR represses arginine synthesis and transport as well as expression of other genes (52), SlyA is an antagonist of H-NS (known to suppress capsule in *K. pneumoniae*) (53, 54), and MprA is a transcriptional regulator with an effect on capsule in uropathogenic *E. coli* (UPEC) (55). Both SlyA and MprA were also shown very recently to be virulence and capsule regulators in *K. pneumoniae* and were renamed KvrA and KvrB (56). SapBCDF has been reported to mediate resistance to antimicrobial peptides (AMPs) in *H. influenzae* by importing them for degradation (57) and was presumed to have this activity in *Enterobacteriaceae* as well, though it has recently been reported that this pump functions as a putrescine exporter in *E. coli* and has no role in AMP resistance (58). ArgR and SapBCDF have not previously been linked to capsule regulation.

To confirm that the alterations in capsule production observed in the NTUH-K2044 $\Delta argR$, $\Delta slyA$, $\Delta mprA$, and $\Delta sapBCDF$ mutants were due to the deleted genes, each mutant was complemented by reintroducing the wild-type gene on the chromosome (see Materials and Methods). Although this complementation strategy ensures wild-type levels of expression, it cannot rule out polar effects. Complementation caused a complete restoration of wild-type capsule production, as measured by the hypermucoidity and uronic acid assays (Fig. 4A and B). To define changes in capsule architecture, each mutant strain was examined by transmission electron microscopy (TEM) (Fig. 4C). Wild-type *K. pneumoniae* NTUH-K2044 had a thick, filamentous capsule of roughly half the cell diameter. The $\Delta argR$ and $\Delta slyA$ mutants had capsules with slightly reduced thickness and finer filaments, while the $\Delta mprA$ mutant had extremely fine and diffuse filaments such that the boundary of the capsule was not clear. The $\Delta sapBCDF$ capsule had some thick filaments but at lower density than NTUH-K2044, with an additional gel-like layer visible outside these filaments. The virulence of the $\Delta argR$, $\Delta slyA$, $\Delta mprA$, and $\Delta sapBCDF$ mutants, and their complements, was assessed by infection of research-grade *Galleria mellonella* larvae, an established invertebrate model for *Klebsiella* infections (59). Each of the reduced-capsule strains showed a virulence defect relative to the wild-type strain which was restored on complementation (Fig. 5A), while the $\Delta sapBCDF$ mutant did not have changed virulence compared to the wild type.

The *sap* transporter alters serum survival but does not affect antimicrobial peptide resistance. We then examined the effect of ArgR, MprA, SlyA, and SapBCDF on resistance to human serum. After 2 h, the NTUH-K2044 wild type showed full survival with a slight increase in viable count, while the *wza* mutant was reduced in viable count by ~25-fold. The $\Delta argR$, $\Delta mprA$, and $\Delta slyA$ mutants did not change significantly (Fig. 5B). The $\Delta sapBCDF$ mutant showed increased viable count compared to the wild-type strain, with a 7-fold increase over the course of the experiment. This increase was unexpected, as the wild-type strain is already fully serum resistant. A double

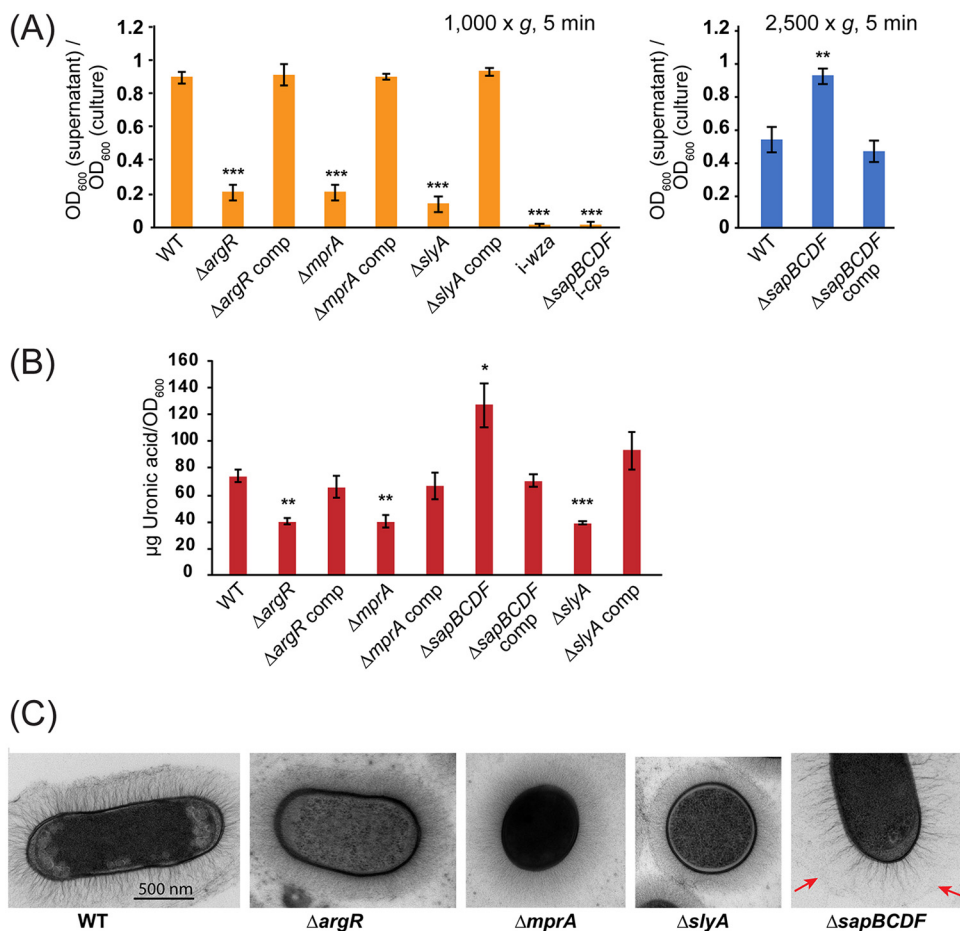


FIG 4 Complementation and electron microscopy of *K. pneumoniae* NTUH-K2044 $\Delta argR$, $\Delta mprA$, $\Delta slyA$, and $\Delta sapBCDF$ mutants. (A) Hypermucoidity assay. Strains were centrifuged at $1,000 \times g$ for 5 min to define decreased hypermucoidity relative to the wild type or at $2,500 \times g$ to identify increases in hypermucoidity relative to the wild type. Significant differences are indicated as follows: **, $P < 0.01$; ***, $P < 0.001$ (one-way ANOVA and Tukey's HSD test). The data represent results from an experiment conducted independently of the experiment whose results are represented in Fig. 3C. comp, complemented. (B) Uronic acid assay to confirm the capsule phenotype of each strain. Differences relative to the wild type were evaluated by pairwise one-way ANOVA with Benjamini-Hochberg correction for multiple testing. *, $P < 0.05$; **, $P < 0.001$; ***, $P < 0.0001$. (C) Transmission electron microscopy images of *K. pneumoniae* NTUH-K2044 and its $\Delta argR$, $\Delta mprA$, $\Delta slyA$, and $\Delta sapBCDF$ mutants. Red arrows indicate the boundary of the gel-like layer of the *sapBCDF* mutant capsule.

$\Delta sapBCDF$ cps mutant was constructed (see Materials and Methods) and showed a drastic reduction in survival, suggesting that the increased serum survival of the NTUH-K2044 $\Delta sapBCDF$ mutant is capsule dependent (Fig. 5B).

We also tested the $\Delta sapBCDF$ mutant for resistance to the peptide antibiotics colistin and polymyxin B. The drug MICs were approximately the same as that seen with the wild type, at $1 \mu g/ml$ for colistin and $0.75 \mu g/ml$ for polymyxin B, indicating that the Sap transporter in *K. pneumoniae* does not contribute to antimicrobial peptide resistance.

sap mutation increases transcription of capsule middle genes without activating the Rcs system. We then wished to determine whether mutation of the Sap transporter increased capsule production by acting on transcription. RNA was extracted from late-exponential-phase wild-type and $\Delta sapBCDF$ cells, and the abundance of three capsule locus transcripts—*manC*, *wcaG*, and *wza*—was measured by reverse transcription real-time quantitative PCR (qRT-PCR). These genes are transcribed from separate promoters. The $\Delta sapBCDF$ mutant showed elevated expression of *wcaG*, at 2.5 times wild-type levels, while expression of *wza* and *manC* was not significantly changed (Fig. 5C).

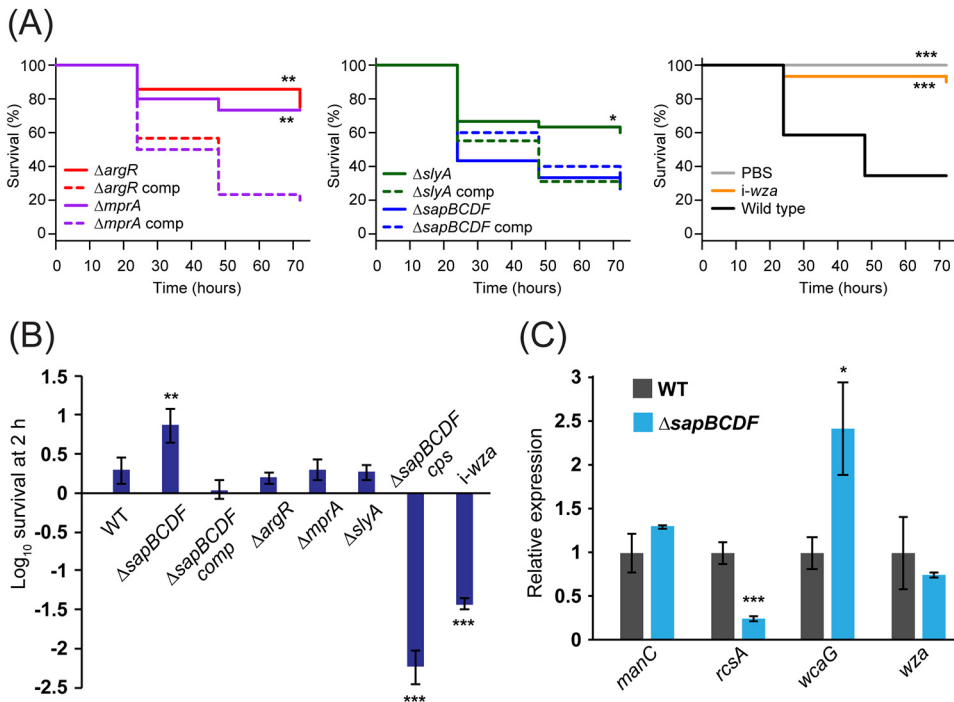


FIG 5 Virulence of selected mutants. (A) Killing of research-grade *Galleria mellonella* larvae by infection with *K. pneumoniae* NTUH-K2044 wild-type or mutant strains. Larvae were infected at an inoculum of 10^5 . Differences in killing compared to the wild type were evaluated using the Kaplan-Meier log rank test and are indicated as follows: *, $P < 0.05$; **, $P < 0.01$; ***, $P < 0.001$. (B) Survival in human serum. Differences relative to the wild type are indicated as follows: **, $P < 0.01$; ***, $P < 0.001$ (pairwise one-way ANOVA). (C) Expression of several capsule-related genes in strain NTUH-K2044 $\Delta sapBCDF$. Transcript abundance was measured using the relative standard curve method with *recA* as a reference gene, and data were normalized to the WT. *, $P < 0.05$; ***, $P < 0.001$ (one-way ANOVA).

The Rcs phosphorelay system regulates capsule expression in *E. coli* and other enterobacteriaceae and is induced by cues such as membrane stress (60, 61). RcsA is a component of the system which autoregulates and increases its own expression when activated. We measured *rcsA* transcript levels to determine whether loss of the $\Delta sapBCDF$ genes induces *rcsA* (Fig. 5C). Unexpectedly, levels of *rcsA* were much lower in the mutant than in the wild type, indicating that Sap-dependent induction of capsule expression does not occur through *rcsA*. Note, however, that RcsA is not required for all permutations of Rcs signaling as RcsB can interact with a number of partner proteins to regulate transcription (60).

Capsule is at the center of a complex regulatory network in *Klebsiella pneumoniae*. We identified numerous putative capsule regulators by density-TraDISort and validated the results of our screen with single-gene-deletion mutants. We propose an integrated model for how the genes we identified may collectively control *K. pneumoniae* NTUH-K2044 capsule. This model is based on our results and previous published work in *K. pneumoniae* and other enterobacteria (particularly *Escherichia coli*). Full details of the literature relevant to each hit are listed in Table S4.

Major nodes for transcriptional control are the CsrB carbon source utilization system and the Rcs phosphorelay system. Each of these systems is itself regulated by multiple genes identified in our study—CsrB integrates signals from the UvrY-BarA two-component system (a capsule down hit) and various carbon metabolic genes, is activated by DksA, and is targeted for degradation by CsrD (a capsule up hit); the Rcs system is induced by MdoGH mutation, can cooperate with RmpA and RmpA2 to induce capsule, and also responds to carbon metabolism and some forms of enterobacterial common antigen. SlyA/KvrA and MprA/KvrB both promote capsule transcription (56). The SlyA/KvrA protein acts as a temperature-dependent switch which acts by

relieving H-NS-mediated transcriptional silencing; H-NS suppressed expression of *rcaA* and the three capsule operons in a clinical *K. pneumoniae* strain of capsule type K39 (53). Capsule is also affected by the composition of the cell envelope, and mutations in *lpp* or various LPS-related genes can reduce the retention of capsule at the cell surface. Note that several genes related to cell envelope composition and membrane stress have been shown to regulate the Rcs system (61); therefore, some of the cell envelope component genes identified in our study may act through RcsB. Our work has also uncovered novel regulators of capsule that, at this stage, cannot be tied to the wider regulatory network, such as *argR*, and the ABC transporter *Sap*. We intend to define the mechanisms by which these genes affect capsule in future studies.

DISCUSSION

We have developed a simple, robust technology for genome-wide studies of bacterial capsule, density-TraDISort, and applied it to identify capsule regulators in two strains of *K. pneumoniae*. In doing so, we have identified multiple positive and negative regulators of capsule production, including several genes not previously linked to capsule in this species.

To our knowledge, this was one of the first studies employing physical selection independently of bacterial survival and growth to separate TraDIS libraries and represents the first time that density-based physical selection has been applied to studying capsule regulation in *K. pneumoniae*. TraDISort/FAST-INSeq technology with fluorescence-based sorting has to date been used to identify genes affecting efflux of ethidium bromide and mutations influencing expression of a *Salmonella enterica* serovar Typhi toxin reporter (48, 62). We have expanded the utility of this method by adding a selection step based on cell density, allowing us to resolve different capsulation states. We envisage that, in addition to facilitating genome-wide screens for altered capsulation in other bacterial species, density-TraDISort could be used to identify genes affecting cell size and shape or cell aggregation.

Our study was the second application of TraDIS to screen for genes affecting bacterial capsule production, following a recent study focused on UPEC (55). The UPEC study utilized a capsule-specific phage to positively select transposon insertion mutants lacking capsule; two novel capsule regulators were identified in this way. Compared with phage-based selection, our method offers increased sensitivity—mutants with a range of capsule phenotypes can be identified, in addition to capsule-null mutations. In addition, there is an option for very stringent selection of hits, as cutoffs can be applied on the basis of both negative selection (loss from the top fraction) and positive selection (enrichment in another fraction). However, density-based selection is less specific to capsule than phage infection, and there is the possibility that mutations could affect cell density in a capsule-independent manner. Interestingly, one of the novel *Klebsiella* capsule regulators identified in this study, *MprA*, was also shown to regulate capsule in UPEC. In *Klebsiella pneumoniae*, this gene increases capsule production above a baseline in hypermuroid strains (56) (Fig. 3A and 4; see also Fig. S4B in the supplemental material), while a UPEC Δ *mprA* mutant did not produce capsule at all.

We have shown that capsule production in *K. pneumoniae* NTUH-K2044 is controlled by many different global regulatory systems, allowing us to provide a detailed snapshot of the control of capsule in this strain (Fig. 6). Note that our assay was performed on bacterial cells at the late-stationary-growth phase, in LB medium, under microaerophilic conditions. This condition was used in this study because the associated level of capsule production is high, offering good resolution for capsule-based selection of mutants. Additional regulators, linked to different cues and stresses, are likely to be involved in different environments. Many of the regulators identified in this study were called as hits only in the hypermuroid strain, *K. pneumoniae* NTUH-K2044. It remains to be seen whether these same regulators control capsule (though to a degree outside the resolution of our gradient) in other *K. pneumoniae* strains; note, though, that several genes of *K. pneumoniae* ATCC 43816 (including *uvrY*, *barA*, *csrB*, *rcaA*, and *rcaB*) met our

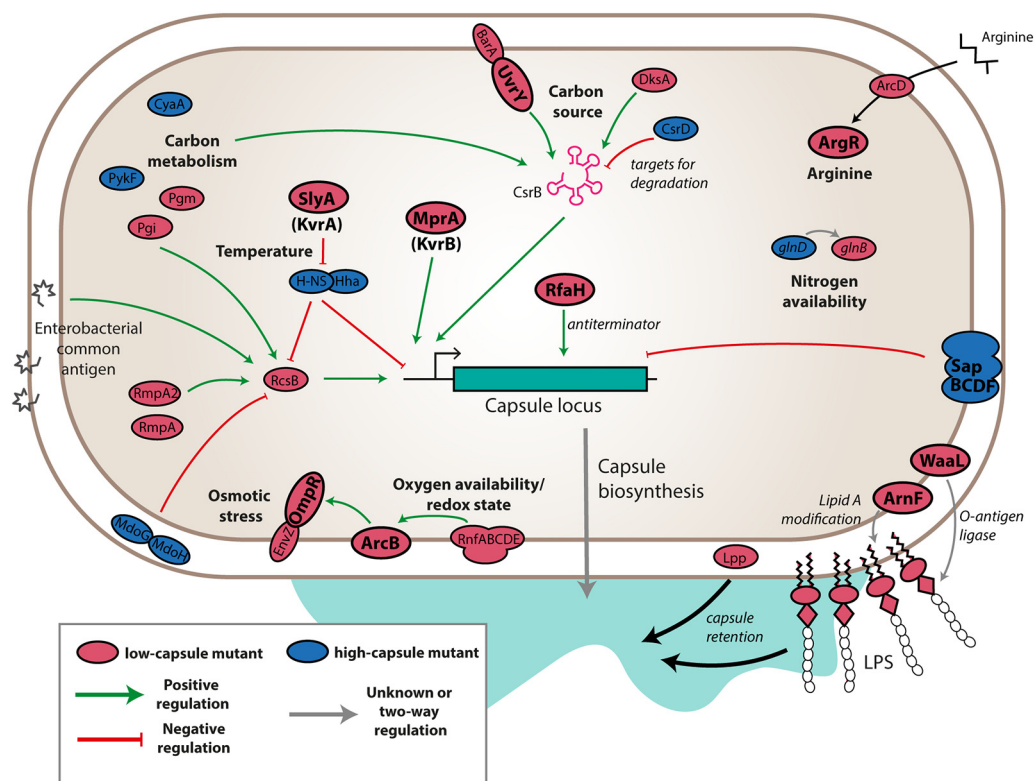


FIG 6 Overview of capsule regulation in NTUH-K2044. Products are colored red for mutants with low capsule and blue for mutants with high capsule, and those genes that were validated in clean deletion knockouts are indicated with bold labels and outlines. Likely modes of action are indicated by green or red arrows for predicted positive and negative effects on transcription of the capsule locus. Gray arrows indicate inputs that may affect capsule synthesis without modulating transcription. Omitted are individual capsule biosynthetic genes, ECA biosynthetic genes, and components of the transcription and translation machinery.

first screening criterion of being lost from the top fraction but not the second of being enriched in the bottom fraction. We speculate that capsule production is subject to complex environmental control across the *Klebsiella* species but that the hypermucoid phenotype is more costly to maintain and more sensitive to disruptions in its regulatory network.

Many of our hits are involved in the synthesis of other cell surface polysaccharides; these included genes for enterobacterial common antigen (ECA), as well as genes for the synthesis or modification of LPS. ECA is a nonimmunogenic surface glycolipid found in various forms in *Enterobacteriaceae*, and structural modifications in this moiety can induce the Rcs system (63, 64). LPS is a major contributor to *K. pneumoniae* pathogenesis in sepsis, though to a lesser extent in pneumonia (12, 18), and various LPS modifications have roles in immune modulation during infection (65, 66). We are confident that the LPS mutations identified in our study affect capsule retention or biosynthesis, rather than density *per se*, because (i) deletion of the O-antigen ligase *waaL* gene did not reduce cell density in an acapsular *K. pneumoniae* NTUH-K2044 strain (Fig. S4A); (ii) some LPS, but not all, biosynthesis genes were hits in our screen; and (iii) the glucuronic acid moieties on the core LPS polysaccharide are required for capsule retention in *K. pneumoniae* (67, 68). In both of the strains that we studied, disrupting genes of the *arn* operon reduced capsulation (Table 1; see also Table S4 in the supplemental material). The *arn* operon has been shown to be responsible for modifying lipid A of LPS with 4-amino-4-deoxy-L-arabinose to mediate resistance to peptide antibiotics (69) but has not previously been linked to capsule. The *arnEF* genes encode a flippase thought to translocate the modified arabinose across the cell membrane (70), while *arnD* is involved in its biosynthesis (71). We hypothesize that the

reduced capsule of mutants of *arnD* and *arnEF* is independent of Lipid A modification, because other genes in this operon did not affect capsule and because a previous study showed that lipid A modification with L-Ara4N does not occur in cells grown in LB (66). Overall, our results hint at a high degree of interdependence among the three major surface polysaccharides of *K. pneumoniae*.

The *sap* ABC transporter, when mutated, was found to promote capsule production by increasing the expression of capsule middle genes (Fig. 3A, 4A and B, and 5C) (Table 1; see also Table S3 and S4). To our knowledge, our study is the first to implicate *sapABCDF* in capsule regulation, though its full functions (or, indeed, the substrate of this transporter in *Klebsiella*) are not known. The *H. influenzae* Sap homologue mediates resistance to antimicrobial peptides by importing them for degradation and is also required for haem uptake (57, 72), while the Sap pump in *E. coli* has been reported to export putrescine and facilitate potassium import through TrkGH (58, 73). We found that the Sap transporter did not affect antimicrobial peptide resistance, which was also observed in *E. coli*. It is unclear how Sap mutation induces *wcaG* while suppressing an important component of the Rcs system—more work will be needed to define the role and mechanism of this transporter in *K. pneumoniae*. For the four mutants characterized in detail in this study, it would be interesting to examine their phenotypes in mammalian models in addition to the invertebrate model used here, to see how these genes influence specific host-pathogen interactions.

We have developed a simple, broadly applicable method for studies of capsulation and used it to define the regulatory network that controls capsule in *K. pneumoniae* NTUH-K2044. We have also identified genes required for full production of capsule in a K2 strain. Although the majority of regulators are located in the core genome of *K. pneumoniae*, there are differences in the specific regulators deployed in the two strains that we investigated, and it would be interesting to determine whether this pattern of strain-specific regulatory networks comprising primarily core genes holds across the *Klebsiella* phylogeny. This intraspecies comparison, together with our data showing that density-based capsule selection can be used in other capsulated bacteria, also opens the possibility for robust interspecies comparisons of capsule regulation.

MATERIALS AND METHODS

Culture conditions and microscopy. *K. pneumoniae* strains were cultured routinely in LB media supplemented with 1.5% (wt/vol) agar as appropriate. Cultures were supplemented with 12.5 μ g/ml chloramphenicol and 12.5 μ g/ml tetracycline when required. *S. pneumoniae* strains were grown on blood agar plates (Oxoid; CM02718) in microaerobic candle jars containing CampyGen sachets at 37°C or in static brain heart infusion (BHI) liquid media (Oxoid; SR0050C). The list of strains, plasmids, and oligonucleotides used in this study is reported in Table S1 in the supplemental material.

Generation of transposon insertion libraries. TraDIS libraries were generated using the mini-Tn5 transposon delivery plasmid pDS1028 (74), introduced into the recipient strain by conjugation. Full details are provided in Text S1 in the supplemental material.

Mutant library fractionation on Percoll gradients. Bacterial mutant libraries were separated on the basis of their capsule expression by centrifugation on a discontinuous Percoll (GE Healthcare) density gradient for 30 min at 3,000 \times *g* (Fig. 1B). Full details are provided in Text S1.

Identification of transposon insertion sites by random-prime PCR. Genomic DNA (gDNA) was prepared from overnight cultures of single reduced-capsule mutants using a DNeasy blood and tissue kit (Qiagen). Random-prime PCR to identify the transposon insertion site in each gDNA template was performed as previously described (75) using primers FS57-59 and FS109 and Herculase II polymerase (Agilent). Amplicons were sequenced using primer FS107.

DNA extraction and next-generation sequencing. Genomic DNA (gDNA) was prepared from each Percoll-resolved fraction by phenol-chloroform extraction. Two micrograms of DNA from each gDNA preparation was used to prepare TraDIS transposon-specific sequencing libraries as described previously, using primer FS108 for specific amplification of transposon junctions (43). Sequencing was carried out on an Illumina MiSeq platform using primer FS107.

Analysis of TraDIS data. The analysis of TraDIS sequencing results was carried out using the Bio-TraDIS pipeline as described previously (43, 44), with minor modifications (see Text S1). All scripts used in this study are available at <https://github.com/sanger-pathogens/Bio-Tradis> and https://github.com/francesca-short/tradis_scripts. Comparisons between fractions were based on normalized read counts per gene. Genes with (i) reduced mutant abundance in the top fraction and (ii) increased mutant abundance in the middle or bottom fraction were called as decreased capsule hits, with thresholds of an absolute change in \log_2 FC of >1 and a *q* value of <0.001 . Increased capsule hits in NTUH-K2044 were defined as those with severely reduced mutant abundance in the middle

fraction ($\log_2FC < -3$; q value < 0.001) without enrichment in the bottom fraction ($\log_2FC < 1$), with genes containing very few reads in any fraction excluded (i.e., the value corresponding to \log_2 counts per million in the top fraction was greater than 4).

Generation of the pan-genome and the method of enrichment analysis are described in Text S1.

Construction of single-gene-deletion strains. Single-gene-knockout mutants were constructed in *K. pneumoniae* by allelic exchange. Upstream and downstream sequences (> 500 bp) for each target gene were amplified and joined by overlap PCR, cloned into pKNG101-Tc, and introduced into the recipient strain by conjugation with the *E. coli* β 2163 donor strain. All primers used, and the resulting constructs, are listed in Table S1. Conjugation patches were incubated for 1 h at 37°C and then for 16 h at 20°C. Single-crossover mutants were selected on LB agar plus 15 μ g/ml tetracycline. Double-crossover mutants were selected on low-salt LB agar plus 5% sucrose at room temperature and were subsequently patched onto LB plus sucrose and LB plus tetracycline plates to confirm loss of the vector. Mutants were confirmed by PCR across the deleted region. Mutants were complemented by reintroduction of the relevant gene into its original location on the chromosome by allelic exchange as described above, using a vector carrying the gene and its flanking region. The Δ sapBCDF cps (*K. pneumoniae* 1_3713 [KP1_3713]) double mutant was generated by random transposon mutagenesis of the Δ sapBCDF strain with the pDS1028 vector, followed by selection of acapsular mutants from the pool by density-gradient centrifugation and random-prime PCR to identify the insertion site.

Quantification of capsule by uronic acid assay. Capsule extraction and quantification of uronic acids were performed as described previously (14, 76), with modifications (see Text S1).

Hypermucoviscosity assay. Cultures of *K. pneumoniae* were grown overnight in 5 ml LB medium at 37°C. These cultures were sedimented at 1,000 $\times g$ or 2,500 $\times g$ for 5 min (room temperature). The optical density at 600 nm (OD_{600}) of the top 500 μ l of supernatant was determined by spectrophotometry. Results were expressed as a ratio of the supernatant OD_{600} to that in the input culture.

Electron microscopy. Colonies were taken directly from an agar plate, frozen at high pressure in a Balzers HP010, and freeze-substituted for 8 h in acetone containing 0.1% tannic acid and 0.5% glutaraldehyde at -90°C followed by 1% osmium tetroxide-acetone for 24 h at -50°C . They were then embedded in Lowicryl HM20 monostep resin. Ultrathin sections were cut on a Leica UC6 ultramicrotome and contrasted by the use of uranyl acetate and lead citrate. Images of bacteria were taken on an FEI Spirit Biotwin 120 kV TEM with a Tietz F4.15 charge-coupled-device (CCD) camera.

Serum resistance assay. Bacteria were grown in LB to an OD_{600} of 1, pelleted, and resuspended in sterile phosphate-buffered saline (PBS). Human sera (Sigma-Aldrich S7023) (400 μ l) was prewarmed to 37°C and added to 200 μ l bacterial suspension, and the mixture was incubated at 37°C for 2 h. Viable bacterial counts were determined before and after incubation.

Galleria mellonella infection. Larvae of *G. mellonella* were purchased from BioSystems Technology Ltd. (United Kingdom) (research-grade larvae) and used within 1 week. Bacteria were grown overnight, subcultured and grown to an OD_{600} of 1, and then resuspended in sterile PBS. Larvae were infected by injecting the bacterial suspension (10^5 cells) into the right hind proleg of the larvae using a Hamilton syringe. Infected larvae were incubated at 37°C and monitored every 24 h and were scored as dead when they were unresponsive to touch. Thirty larvae were used per strain, and these were infected in three batches of 10 using replicate cultures.

Antimicrobial peptide resistance tests. Strains were grown overnight, subcultured, and grown to an OD_{600} of 1.0. This culture (100 μ l) was spread on the surface of an LB agar plate and dried, and an Etest (bioMérieux) strip was placed on the surface of the plate. Plates were incubated face up at 37°C, and the result was read after 6 h to avoid overgrowth of the capsule interfering with the reading.

RNA extraction and qRT-PCR. Bacteria were grown in LB medium at 37°C to an OD_{600} of 1.0. Cultures were mixed with 2 \times volumes of RNAProtect reagent, centrifuged, and RNA extracted using a MasterPure Complete DNA and RNA purification kit (Epicentre) according to the manufacturer's instructions. Samples were then subjected to in-solution DNase I digestion (Qiagen) and cleaned up using a Qiagen RNeasy minikit. Reverse transcription of 200 ng RNA was performed using ProtoScriptII enzyme (NEB) per the supplied instructions.

Transcripts were quantified using a StepOne real-time PCR instrument with a Kapa SYBR FAST qPCR kit. Relative abundances were determined using the relative standard curve method with *K. pneumoniae* NTUH-K2044 gDNA as a standard and *recA* as the reference gene (77).

Accession number(s). Sequences generated during this study have been deposited into the European Nucleotide Archive (ENA; <http://www.ebi.ac.uk/ena>) under study accession number ERP105653.

SUPPLEMENTAL MATERIAL

Supplemental material for this article may be found at <https://doi.org/10.1128/mBio.01863-18>.

TEXT S1, DOCX file, 0.03 MB.

FIG S1, JPG file, 0.3 MB.

FIG S2, JPG file, 0.3 MB.

FIG S3, JPG file, 0.4 MB.

FIG S4, JPG file, 0.1 MB.

TABLE S1, DOCX file, 0.02 MB.

TABLE S2, XLSX file, 0.04 MB.

TABLE S3, XLSX file, 1.2 MB.

TABLE S4, XLSX file, 0.05 MB.

TABLE S5, XLSX file, 0.04 MB.

ACKNOWLEDGMENTS

We thank Matt Mayo, Jacqui Brown, and the sequencing teams at the Wellcome Sanger Institute for TraDIS sequencing and the Pathogen Informatics team for advice on the analysis. We also thank Susannah Salter, Nick Croucher, George Salmond, Rita Monson, Jose Bengochea, and Jin-Town Wang for supplying strains and plasmids.

This work was supported by Wellcome (grant 206194). M.J.D. is supported by a Wellcome Sanger Institute PhD Studentship. F.L.S. is supported by a Sir Henry Wellcome postdoctoral fellowship (grant 106063/A/14/Z).

REFERENCES

- Podschun R, Ullmann U. 1998. *Klebsiella* spp. as nosocomial pathogens: epidemiology, taxonomy, typing methods, and pathogenicity factors. *Clin Microbiol Rev* 11:589–603.
- Holt KE, Wertheim H, Zadoks RN, Baker S, Whitehouse CA, Dance D, Jenney A, Connor TR, Hsu LY, Severin J, Brisse S, Cao H, Wilksch J, Gorrie C, Schultz MB, Edwards DJ, Nguyen KV, Nguyen TV, Dao TT, Mensink M, Minh VL, Nhu NTK, Schultz C, Kuntaman K, Newton PN, Moore CE, Strugnell RA, Thomson NR. 2015. Genomic analysis of diversity, population structure, virulence, and antimicrobial resistance in *Klebsiella pneumoniae*, an urgent threat to public health. *Proc Natl Acad Sci* 112: E3574–E3581. <https://doi.org/10.1073/pnas.1501049112>.
- Broberg CA, Palacios M, Miller VL. 2014. *Klebsiella*: a long way to go towards understanding this enigmatic jet-setter. *F1000Prime Rep* 6:64. <https://doi.org/10.12703/P6-64>.
- Maroncle N, Rich C, Forestier C. 2006. The role of *Klebsiella pneumoniae* urease in intestinal colonization and resistance to gastrointestinal stress. *Res Microbiol* 157:184–193. <https://doi.org/10.1016/j.resmic.2005.06.006>.
- Sahly H, Podschun R, Ullmann U. 2002. *Klebsiella* infections in the immunocompromised host, p 237–249. In Keisari Y, Ofek I (ed), *The biology and pathology of innate immunity mechanisms*. Springer US, Boston, MA.
- Shon AS, Bajwa RPS, Russo TA. 2013. Hypervirulent (hypermucoviscous) *Klebsiella pneumoniae*. *Virulence* 4:107–118. <https://doi.org/10.4161/viru.22718>.
- Gomez-Simmonds A, Uhlemann A-C. 2017. Clinical implications of genomic adaptation and evolution of carbapenem-resistant *Klebsiella pneumoniae*. *J Infect Dis* 215:518–527. <https://doi.org/10.1093/infdis/jiw378>.
- Wang JH, Liu YC, Lee SS, Yen MY, Chen YS, Wang JH, Wann SR, Lin HH. 1998. Primary liver abscess due to *Klebsiella pneumoniae* in Taiwan. *Clin Infect Dis* 26:1434–1438. <https://doi.org/10.1086/516369>.
- Pomakova DK, Hsiao C-B, Beanan JM, Olson R, MacDonald U, Keynan Y, Russo TA. 2012. Clinical and phenotypic differences between classic and hypervirulent *Klebsiella pneumoniae*: an emerging and under-recognized pathogenic variant. *Eur J Clin Microbiol Infect Dis* 31:981–989. <https://doi.org/10.1007/s10096-011-1396-6>.
- Cheng D-L, Liu Y-C, Yen M-Y, Liu C-Y, Wang R-S. 1991. Septic metastatic lesions of pyogenic liver abscess: their association with *Klebsiella pneumoniae* bacteremia in diabetic patients. *Arch Intern Med* 151:1557–1559. <https://doi.org/10.1001/archinte.1991.00400080059010>.
- Fang C-T, Lai S-Y, Yi W-C, Hsueh P-R, Liu K-L, Chang S-C. 2007. *Klebsiella pneumoniae* genotype K1: an emerging pathogen that causes septic ocular or central nervous system complications from pyogenic liver abscess. *Clin Infect Dis* 45:284–293. <https://doi.org/10.1086/519262>.
- Paczosa MK, Meccas J. 2016. *Klebsiella pneumoniae*: going on the offense with a strong defense. *Microbiol Mol Biol Rev* 80:629–661. <https://doi.org/10.1128/MMBR.00078-15>.
- Struve C, Forestier C, Krogfelt KA. 2003. Application of a novel multi-screening signature-tagged mutagenesis assay for identification of *Klebsiella pneumoniae* genes essential in colonization and infection. *Microbiology* 149:167–176. <https://doi.org/10.1099/mic.0.25833-0>.
- Favre-Bonté S, Licht TR, Forestier C, Krogfelt KA. 1999. *Klebsiella pneumoniae* capsule expression is necessary for colonization of large intestines of streptomycin-treated mice. *Infect Immun* 67:6152–6156.
- Hsu C-R, Lin T-L, Chen Y-C, Chou H-C, Wang J-T. 2011. The role of *Klebsiella pneumoniae rmpA* in capsular polysaccharide synthesis and virulence revisited. *Microbiology* 157:3446–3457. <https://doi.org/10.1099/mic.0.050336-0>.
- Cheng HY, Chen YS, Wu CY, Chang HY, Lai YC, Peng HL. 2010. RmpA regulation of capsular polysaccharide biosynthesis in *Klebsiella pneumoniae* CG43. *J Bacteriol* 192:3144–3158. <https://doi.org/10.1128/JB.00031-10>.
- Wyres KL, Wick RR, Gorrie C, Jenney A, Follador R, Thomson NR, Holt KE. 2016. Identification of *Klebsiella* capsule synthesis loci from whole genome data. *Microb Genom* 2:e000102. <https://doi.org/10.1099/mgen.0.000102>.
- Cortés G, Borrell N, de Astorza B, Gómez C, Saulea J, Albertí S. 2002. Molecular analysis of the contribution of the capsular polysaccharide and the lipopolysaccharide O side chain to the virulence of *Klebsiella pneumoniae* in a murine model of pneumonia. *Infect Immun* 70: 2583–2590. <https://doi.org/10.1128/IAI.70.5.2583-2590.2002>.
- Patel PK, Russo TA, Karchmer AW. 2014. Hypervirulent *Klebsiella pneumoniae*. *Open Forum Infect Dis* 1:ofu028. <https://doi.org/10.1093/ofid/ofu028>.
- Nassif X, Sansonetti PJ. 1986. Correlation of the virulence of *Klebsiella pneumoniae* K1 and K2 with the presence of a plasmid encoding aerobactin. *Infect Immun* 54:603–608.
- Chen Y-TT, Chang H-YY, Lai Y-CC, Pan C-CC, Tsai S-FF, Peng H-LL. 2004. Sequencing and analysis of the large virulence plasmid pLVPK of *Klebsiella pneumoniae* CG43. *Gene* 337:189–198. <https://doi.org/10.1016/j.gene.2004.05.008>.
- Mizuta K, Ohta M, Mori M, Hasegawa T, Nakashima I, Kato N. 1983. Virulence for mice of *Klebsiella* strains belonging to the O1 group: relationship to their capsular (K) types. *Infect Immun* 40:56–61.
- Nassif X, Fournier JM, Arondel J, Sansonetti PJ. 1989. Mucoid phenotype of *Klebsiella pneumoniae* is a plasmid-encoded virulence factor. *Infect Immun* 57:546–552.
- Yeh K-M, Kurup A, Siu LK, Koh YL, Fung C-P, Lin J-C, Chen T-L, Chang F-Y, Koh T-H. 2007. Capsular serotype K1 or K2, rather than *magA* and *rmpA*, is a major virulence determinant for *Klebsiella pneumoniae* liver abscess in Singapore and Taiwan. *J Clin Microbiol* 45:466–471. <https://doi.org/10.1128/JCM.01150-06>.
- Russo TA, Shon AS, Beanan JM, Olson R, MacDonald U, Pomakov AO, Visitation MP. 2011. Hypervirulent *K. pneumoniae* secretes more and more active iron-acquisition molecules than “classical” *K. pneumoniae* thereby enhancing its virulence. *PLoS One* 6:e26734. <https://doi.org/10.1371/journal.pone.0026734>.
- Yeh K-M, Lin J-C, Yin F-Y, Fung C-P, Hung H-C, Siu L-K, Chang F-Y. 2010. Revisiting the importance of virulence determinant *magA* and its surrounding genes in *Klebsiella pneumoniae* causing pyogenic liver abscesses: exact role in serotype K1 capsule formation. *J Infect Dis* 201:1259–1267. <https://doi.org/10.1086/606010>.
- Fang C-T, Lai S-Y, Yi W-C, Hsueh P-R, Liu K-L. 2010. The function of *wzy_K1* (*magA*), the serotype K1 polymerase gene in *Klebsiella pneumoniae cps* gene cluster. *J Infect Dis* 201:1268–1269. <https://doi.org/10.1086/652183>.

28. Fang C-T, Chuang Y-P, Shun C-T, Chang S-C, Wang J-T. 2004. A novel virulence gene in *Klebsiella pneumoniae* strains causing primary liver abscess and septic metastatic complications. *J Exp Med* 199:697–705. <https://doi.org/10.1084/jem.20030857>.
29. Lai Y-C, Peng H-L, Chang H-Y. 2003. RmpA2, an activator of capsule biosynthesis in *Klebsiella pneumoniae* CG43, regulates K2 cps gene expression at the transcriptional level. *J Bacteriol* 185:788–800. <https://doi.org/10.1128/JB.185.3.788-800.2003>.
30. Yu W-L, Ko W-C, Cheng K-C, Lee C-C, Lai C-C, Chuang Y-C. 2008. Comparison of prevalence of virulence factors for *Klebsiella pneumoniae* liver abscesses between isolates with capsular K1/K2 and non-K1/K2 serotypes. *Diagn Microbiol Infect Dis* 62:1–6. <https://doi.org/10.1016/j.diagmicrobio.2008.04.007>.
31. Kobayashi SD, Porter AR, Freedman B, Pandey R, Chen L, Kreiswirth BN, Deleo R. 2018. Antibody-mediated killing of carbapenem-resistant ST258 *Klebsiella pneumoniae* by human neutrophils. *mBio* 9:e00297-18. <https://doi.org/10.1128/mBio.00297-18>.
32. Diago-Navarro E, Motley M, Ruiz-Perez G, Yu W, Austin J, Seco B, Xiao G, Chikhalya A, Seeberger PH, Fries BC. 2018. Novel, broadly reactive anticapsular antibodies against carbapenem-resistant *Klebsiella pneumoniae* protect from infection. *mBio* 9:e00091-18. <https://doi.org/10.1128/mBio.00091-18>.
33. Lin TL, Hsieh PF, Huang YT, Lee WC, Tsai YT, Su PA, Pan YJ, Hsu CR, Wu MC, Wang JT. 2014. Isolation of a bacteriophage and its depolymerase specific for K1 capsule of *Klebsiella pneumoniae*: implication in typing and treatment. *J Infect Dis* 210:1734–1744. <https://doi.org/10.1093/infdis/jiu332>.
34. Pan YJ, Lin TL, Lin YT, Su PA, Chen CT, Hsieh PF, Hsu CR, Chen CC, Hsieh YC, Wang JT. 2015. Identification of capsular types in carbapenem-resistant *Klebsiella pneumoniae* strains by wzc sequencing and implications for capsule depolymerase treatment. *Antimicrob Agents Chemother* 59:1038–1047. <https://doi.org/10.1128/AAC.03560-14>.
35. Hsieh PF, Lin HH, Lin TL, Chen YY, Wang JT. 2017. Two T7-like bacteriophages, K5-2 and K5-4, each encodes two capsule depolymerases: isolation and functional characterization. *Sci Rep* 7:4624. <https://doi.org/10.1038/s41598-017-04644-2>.
36. Navon-Venezia S, Kondratyeva K, Carattoli A. 2017. *Klebsiella pneumoniae*: a major worldwide source and shuttle for antibiotic resistance. *FEMS Microbiol Rev* 41:252–275. <https://doi.org/10.1093/fems/rev/fux013>.
37. Yu W-L, Ko W-C, Cheng K-C, Lee H-C, Ke D-S, Lee C-C, Fung C-P, Chuang Y-C. 2006. Association between rmpA and magA genes and clinical syndromes caused by *Klebsiella pneumoniae* in Taiwan. *Clin Infect Dis* 42:1351–1358. <https://doi.org/10.1086/503420>.
38. Bachman MA, Breen P, Deornellas V, Mu Q, Zhao L, Wu W, Cavalcoli JD, Mobley HLT. 2015. Genome-wide identification of *Klebsiella pneumoniae* fitness genes during lung infection. *mBio* 6:e00775. <https://doi.org/10.1128/mBio.00775-15>.
39. Gottesman S, Trisler P, Torres-Cabassa A. 1985. Regulation of capsular polysaccharide synthesis in *Escherichia coli* K-12: characterization of three regulatory genes. *J Bacteriol* 162:1111–1119.
40. Stout V, Torres-Cabassa A, Maurizi MR, Gutnick D, Gottesman S. 1991. RcsA, an unstable positive regulator of capsular polysaccharide synthesis. *J Bacteriol* 173:1738–1747. <https://doi.org/10.1128/jb.173.5.1738-1747.1991>.
41. McCallum KL, Whitfield C. 1991. The rcsA gene of *Klebsiella pneumoniae* O1:K20 is involved in expression of the serotype-specific K (capsular) antigen. *Infect Immun* 59:494–502.
42. Lin CT, Wu CC, Chen YS, Lai YC, Chi C, Lin JC, Chen Y, Peng HL. 2011. Fur regulation of the capsular polysaccharide biosynthesis and iron-acquisition systems in *Klebsiella pneumoniae* CG43. *Microbiology* 157:419–429. <https://doi.org/10.1099/mic.0.044065-0>.
43. Barquist L, Mayho M, Cummins C, Cain AK, Boinett CJ, Page AJ, Langridge GC, Quail MA, Keane JA, Parkhill J. 2016. The TraDIS toolkit: sequencing and analysis for dense transposon mutant libraries. *Bioinformatics* 32:1109–1111. <https://doi.org/10.1093/bioinformatics/btw022>.
44. Langridge GC, Phan MD, Turner DJ, Perkins TT, Parts L, Haase J, Charles I, Maskell DJ, Peters SE, Dougan G, Wain J, Parkhill J, Turner KA. 2009. Simultaneous assay of every *Salmonella* Typhi gene using one million transposon mutants. *Genome Res* 19:2308–2316. <https://doi.org/10.1101/gr.097097.109>.
45. Patrick S, Reid JH. 1983. Separation of capsulate and non-capsulate *Bacteroides fragilis* on a discontinuous density gradient. *J Med Microbiol* 16:239–241. <https://doi.org/10.1099/00222615-16-2-239>.
46. Menck K, Behme D, Pantke M, Reiling N, Binder C, Pukrop T, Klemm F. 2014. Isolation of human monocytes by double gradient centrifugation and their differentiation to macrophages in Teflon-coated cell culture bags. *J Vis Exp* 2014:e51554. <https://doi.org/10.3791/51554>.
47. Brunner J, Scheres N, El Idrissi NB, Deng DM, Laine ML, van Winkelhoff AJ, Crielaard W. 2010. The capsule of *Porphyromonas gingivalis* reduces the immune response of human gingival fibroblasts. *BMC Microbiol* 10:5. <https://doi.org/10.1186/1471-2180-10-5>.
48. Hassan KA, Cain AK, Huang T, Liu Q, Elbourne LDH, Boinett CJ, Brzoska AJ, Li L, Ostrowski M, Nhu NTK, Nhu TDH, Baker S, Parkhill J, Paulsen IT, Thi N, Nhu K, Do T, Nhu H, Baker S, Parkhill J, Paulsen IT. 2016. Fluorescence-based flow sorting in parallel with transposon insertion site sequencing identifies multidrug efflux systems in *Acinetobacter baumannii*. *mBio* 7:e01200-16. <https://doi.org/10.1128/mBio.01200-16>.
49. Alexa A, Rahnenfuhrer J. 2016. topGO: enrichment analysis for gene ontology. R package version 2.32.0. <https://bioconductor.org/packages/release/bioc/html/topGO.html>.
50. Grossmann S, Bauer S, Robinson PN, Vingron M. 2007. Improved detection of overrepresentation of Gene-Ontology annotations with parent-child analysis. *Bioinformatics* 23:3024–3031. <https://doi.org/10.1093/bioinformatics/btm440>.
51. Malinverni JC, Silhavy TJ. 2009. An ABC transport system that maintains lipid asymmetry in the Gram-negative outer membrane. *Proc Natl Acad Sci U S A* 106:8009–8014. <https://doi.org/10.1073/pnas.0903229106>.
52. Cho B-K, Federowicz S, Park Y-S, Zengler K, Pálsson BØ. 2011. Deciphering the regulatory logic of a stimulon. *Nat Chem Biol* 8:65–71. <https://doi.org/10.1038/nchembio.710>.
53. Ares MA, Fernández-Vázquez JL, Rosales-Reyes R, Jarillo-Quijada MD, von Bargen K, Torres J, González-y-Merchand JA, Alcántar-Curiel MD, De la Cruz MA. 2016. H-NS nucleoid protein controls virulence features of *Klebsiella pneumoniae* by regulating the expression of type 3 pili and the capsule polysaccharide. *Front Cell Infect Microbiol* 6:13. <https://doi.org/10.3389/fcimb.2016.00013>.
54. Corbett D, Bennett HJ, Askar H, Green J, Roberts IS. 2007. SlyA and H-NS regulate transcription of the *Escherichia coli* K5 capsule gene cluster, and expression of slyA in *Escherichia coli* is temperature-dependent, positively autoregulated, and independent of H-NS. *J Biol Chem* 282:33326–33335. <https://doi.org/10.1074/jbc.M703465200>.
55. Goh KKG, Phan M-D, Forde BM, Chong TM, Yin W-F, Chan K-G, Ulett GC, Sweet MJ, Beatson SA, Schembri MA. 2017. Genome-wide discovery of genes required for capsule production by uropathogenic *Escherichia coli*. *mBio* 8:e01558-17. <https://doi.org/10.1128/mBio.01558-17>.
56. Palacios M, Miner TA, Frederick DR, Sepulveda VE, Quinn JD, Walker KA, Miller VL. 2018. Identification of two regulators of virulence that are conserved in *Klebsiella pneumoniae* classical and hypervirulent strains. *mBio* 9:e01443-18.
57. Gruenheid S, Le Moual H. 2012. Resistance to antimicrobial peptides in Gram-negative bacteria. *FEMS Microbiol Lett* 330:81–89. <https://doi.org/10.1111/j.1574-6968.2012.02528.x>.
58. Sugiyama Y, Nakamura A, Matsumoto M, Kanbe A, Sakanaka M, Higashi K, Igarashi K, Katayama T, Suzuki H, Kurihara S. 2016. A novel putrescine exporter SapBCDF of *Escherichia coli*. *J Biol Chem* 291:26343–26351. <https://doi.org/10.1074/jbc.M116.762450>.
59. Insua JL, Llobet E, Moranta D, Pérez-Gutiérrez C, Tomás A, Garmendia J, Bengoechea JA. 2013. Modeling *Klebsiella pneumoniae* pathogenesis by infection of the wax moth *Galleria mellonella*. *Infect Immun* 81:3552–3565. <https://doi.org/10.1128/IAI.00391-13>.
60. Wall E, Majdalani N, Gottesman S. 2018. The complex Rcs regulatory cascade. *Annu Rev Microbiol* 72:111–139. <https://doi.org/10.1146/annurev-micro-090817-062640>.
61. Majdalani N, Gottesman S. 2005. The Rcs phosphorelay: a complex signal transduction system. *Annu Rev Microbiol* 59:379–405. <https://doi.org/10.1146/annurev.micro.59.050405.101230>.
62. Fowler CC, Galán JE. 2018. Decoding a *Salmonella* Typhi regulatory network that controls typhoid toxin expression within human cells. *Cell Host Microbe* 23:65–76.e6. <https://doi.org/10.1016/j.chom.2017.12.001>.
63. Castell ME, Vescovi EG. 2011. The Rcs signal transduction pathway is triggered by enterobacterial common antigen structure alterations in *Serratia marcescens*. *J Bacteriol* 193:63–74. <https://doi.org/10.1128/JB.00839-10>.
64. Gozdiewicz TK, Lugowski C, Lukaszewicz J. 2014. First evidence for a covalent linkage between enterobacterial common antigen and lipopolysaccharide in *Shigella sonnei* phase II ECALPS. *J Biol Chem* 289:2745–2754. <https://doi.org/10.1074/jbc.M113.512749>.

65. Mills G, Dumigan A, Kidd T, Hopley L, Bengoechea JA. 2017. Identification and characterization of *Klebsiella pneumoniae* two lpxL lipid A late acyltransferases and their role in virulence. *Infect Immun* 85:e00068-17. <https://doi.org/10.1128/IAI.00068-17>.
66. Llobet E, Martínez-Moliner V, Moranta D, Dahlström KM, Regueiro V, Tomás A, Cano V, Pérez-Gutiérrez C, Frank CG, Fernández-Carrasco H, Insua JL, Salminen TA, Garmendia J, Bengoechea JA. 2015. Deciphering tissue-induced *Klebsiella pneumoniae* lipid A structure. *Proc Natl Acad Sci U S A* 112:E6369–E6378. <https://doi.org/10.1073/pnas.1508820112>.
67. Fresno S, Jiménez N, Izquierdo L, Merino S, Corsaro MM, De CC, Parrilli M, Naldi T, Regué M, Tomás JM, Fresno S, Jime N, Corsaro MM, Castro C, De PM, Toma JM, Naldi T, Regue M, Toma JM, li F, Universitario C. 2006. The ionic interaction of *Klebsiella pneumoniae* K2 capsule and core lipopolysaccharide. *Microbiology* 152:1807–1818. <https://doi.org/10.1099/mic.0.28611-0>.
68. Fresno S, Jiménez N, Canals R, Merino S, Corsaro MM, Lanzetta R, Parrilli M, Pieretti G, Regué M, Tomás JM. 2007. A second galacturonic acid transferase is required for core lipopolysaccharide biosynthesis and complete capsule association with the cell surface in *Klebsiella pneumoniae*. *J Bacteriol* 189:1128–1137. <https://doi.org/10.1128/JB.01489-06>.
69. Olaitan AO, Morand S, Rolain JM. 2014. Mechanisms of polymyxin resistance: acquired and intrinsic resistance in bacteria. *Front Microbiol* 5:643. <https://doi.org/10.3389/fmicb.2014.00643>.
70. Yan A, Guan Z, Raetz CRH. 2007. An undecaprenyl phosphate-aminoarabinose flippase required for polymyxin resistance in *Escherichia coli*. *J Biol Chem* 282:36077–36089. <https://doi.org/10.1074/jbc.M706172200>.
71. Breazeale SD, Ribeiro AA, McClarren AL, Raetz CRH. 2005. A formyltransferase required for polymyxin resistance in *Escherichia coli* and the modification of lipid A with 4-amino-4-deoxy-L-arabinose: identification and function of UDP-4-deoxy-4-formamido-L-arabinose. *J Biol Chem* 280:14154–14167. <https://doi.org/10.1074/jbc.M414265200>.
72. Mason KM, Raffel FK, Ray WC, Bakaletz LO. 2011. Heme utilization by nontypeable *Haemophilus influenzae* is essential and dependent on Sap transporter function. *J Bacteriol* 193:2527–2535. <https://doi.org/10.1128/JB.01313-10>.
73. Harms C, Domoto Y, Celik C, Rahe E, Stumpe S, Schmid R, Nakamura T, Bakker EP. 2001. Identification of the ABC protein SapD as the subunit that confers ATP dependence to the K⁺-uptake systems TrkH and TrkG from *Escherichia coli* K-12. *Microbiology* 147:2991–3003. <https://doi.org/10.1099/00221287-147-11-2991>.
74. Monson R, Smith DS, Matilla MA, Roberts K, Richardson E, Drew A, Williamson N, Ramsay J, Welch M, Salmond GPC. 2015. A plasmid-transposon hybrid mutagenesis system effective in a broad range of Enterobacteria. *Front Microbiol* 6:1442. <https://doi.org/10.3389/fmicb.2015.01442>.
75. Fineran PC, Everson L, Slater H, Salmond GPC. 2005. A GntR family transcriptional regulator (PigT) controls gluconate-mediated repression and defines a new, independent pathway for regulation of the tripyrrole antibiotic, prodigiosin, in *Serratia*. *Microbiology* 151:3833–3845. <https://doi.org/10.1099/mic.0.28251-0>.
76. Lawlor MS, Hsu J, Rick PD, Miller VL. 2005. Identification of *Klebsiella pneumoniae* virulence determinants using an intranasal infection model. *Mol Microbiol* 58:1054–1073. <https://doi.org/10.1111/j.1365-2958.2005.04918.x>.
77. Érika A, Gomes I, Stuchi LP, Maria N, Siqueira G, Henrique JB, Vicentini R, Ribeiro ML, Darrieux M. 2018. Selection and validation of reference genes for gene expression studies in *Klebsiella pneumoniae* using reverse transcription quantitative real-time PCR. *Sci Rep* 8:9001. <https://doi.org/10.1038/s41598-018-27420-2>.